Materials Characterization 126 (2017) 144–148

Contents lists available at ScienceDirect

Materials Characterization

journal homepage: www.elsevier.com/locate/matchar

Characterisation of solidification using combined confocal scanning laser microscopy with infrared thermography

Carl Slater *, Kateryna Hechu, Seetharaman Sridhar

University of Warwick, United Kingdom

ARTICLE INFO

Article history:
Received 11 January 2017
Accepted 26 February 2017
Available online 28 February 2017

Keywords:
Solidification
Thermography
In-situ
Casting

ABSTRACT

Confocal scanning laser microscopy is a growing technique as it offers the unique capability to observe (amongst other things) the solidification of high melting point materials such as steels. Here this technique has been expanded to incorporate an infrared thermographer to gain bulk information about solidification of both pure iron and a low carbon steel. This technique shows a clear indication of the onset and competition of solidification at rates up to 10 °C/s and as such becomes more applicable to the rates expected during steel casting compared to conventional calorimetry.

1. Introduction

With the ever increasing drive to lower emissions and increase efficiency then fabrication of metallic alloys has moved to more novel methods. This can be seen in industries such as aluminium sheet fabrication where companies such as Alcoa have used modern belt casting techniques to reduce production times from days to minutes [1]. This is also seen in the steel industry where belt casting and twin rolling technologies are emerging [2,3]. With these new technologies comes new scientific challenges. One of the specific challenges related to these technologies is that due to the accelerated manufacturing of these products, an acceleration in the solidification rate is seen, and this can have a significant impact on the resultant microstructure.

With regards to steelmaking, conventional continuous casting has been in implementation since the 1970s [2] and although offering the capability to make semi-finished product continuously, solidification rates remained slow and comparable to its ingot casting counterpart (bulk solidification rates of <1 °C/s [4]). For this, conventional techniques for analysing solidification such as Differential Scanning Calorimetry (DSC) were sufficient. However, these newer steelmaking techniques involve much faster cooling rates (belt casting for example shows up to 50 °C/s), and are beyond the capability of DSC (typically around 0.1–0.5 °C/s).

Confocal scanning laser microscope has been shown to offer a greater control over thermal profiles compared to other analytic machines (heating and cooling rates of >50 °C/s can be achieved [5], in addition to this the CSLM is capable of imaging the specimen and offer good environmental control over the DSC. Although optically many physical transformations can be seen in the CSLM, there is merit in being able to define transformations through latent heat of transformation, as optically it relies heavily on the quality of the surface (which is dictated by the atmosphere, type of phase(s) formed during solidification, inclusions present). Visual imaging through CSLM relies on the appearances of surface relief structures on the surface causing topological variances. When these are subtle due to slow transformation rates or rapid surface diffusion smoothing out features on the surface it becomes hard to quantify the evolution. The objective of this work is to establish if thermal imaging in conjuncture with visual observation can be used to enhance the capabilities of the CSLM.

2. Experimental

2.1. Adaption of the CSLM to image using infrared thermography

Use of high temperature CSLM, pioneered by Emi and co-workers at Tohoku University [6–8], and the mechanism of how it works has been documented and explained in detail in literature [5,9–15]. Fig. 1 shows a schematic of the set up used in this report. The CSLM used in this work is a Yonekura VL2000DX-SVF17SP. In a conventional CSLM setup a He-Ne laser is used as an imagining source, however the method proposed here allows the laser to be quickly switched for Infrared Thermographer (IRT).

IRTs typically operate at one of two frequency ranges, either around 1–1.5 μm or 8–14 μm. The halogen bulb used as a heat source in this set up operates at a frequency 300–2000 nm, therefore any imaging source that is used needs to operate at frequencies higher than 2 μm.

The viewing window is conventionally fabricated from quartz due to its thermal stability and high transmissivity around the laser operating frequency. However, quartz transmissivity drops significantly after

* Corresponding author.
E-mail address: c.d.slater@warwick.ac.uk (C. Slater).

http://dx.doi.org/10.1016/j.matchar.2017.02.025
1044-5803/

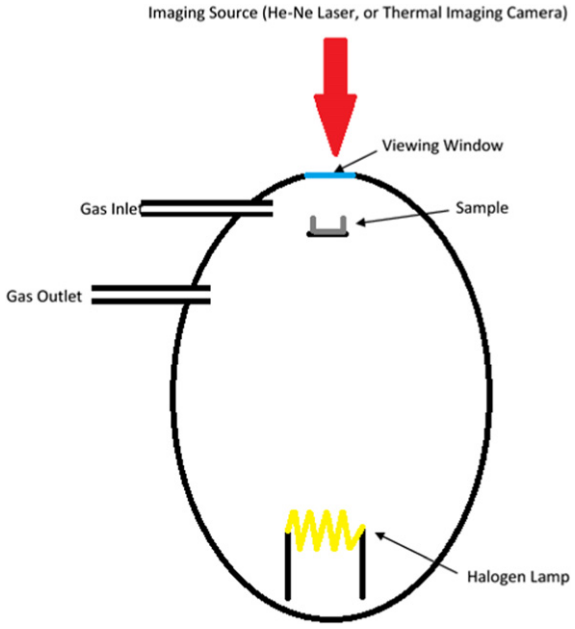

Fig. 1. Schematic diagram showing the experimental set up of the confocal scanning laser microscope.

4 μm. Therefore, for this experimental procedure a CaF_2 window was used which maintains >70% transmissivity up to 14 μm which allowed the usage of a Micro Epsilon TIM 160 thermal imaging camera operating at a frequency of 7.6–13 μm, recording at 120 Hz with a resolution of 160 × 120 pixels using a 6° lens. This camera has a thermal sensitivity of 0.04 K.

The thermographer is clamped 45 mm above the viewing window (allowing air flow around the lens prevents overheating and warping). The camera is then manually focused to the surface of the sample. Radiated heat was calculated by the following equation:

$$\frac{Q}{A} = \varepsilon\sigma T^4$$

where Q is the heat transfer per unit time, σ is the Stefan-Boltzmann constant, T is the absolute temperature and ε is the emissivity of the sample. A value for ε of 0.3 was used for this study which is consistent with liquid steel, this provides an effective temperature which is then used in this equation. The thermographer receives an IR signal from the sample which corresponds to specific energy values, the software then automatically converts this to a temperature for a given emissivity. Therefore, back calculating this means that the accuracy of emissivity is less important, it is only the apparent temperature at a specified emissivity that is needed. This reduces the noise significantly. The spot size used in this study was 0.059 mm^2.

2.2. Solidification trials

Prior to testing the CSLM is calibrated using four pure metals (Al, Au, Ni and Fe) of the same geometry, and heated to 100 °C below the expected melting point at 10 °C/s. The sample is then heated at 0.5 °C/s, and the melting points are verified. This process is repeated three times for each element.

For these trials an electrolytically pure iron (99.999% Fe) and a low carbon steel (0.042C, 0.234Mn) were chosen. Samples of each material were sectioned down to 3 mm cubes and placed in an alumina crucible. The CSLM chamber was then evacuated and backfilled with N6 argon three times before starting each test using a flow rate of 300 mL/min.

Samples were initially heated to 200 °C for 2 min to dry the sample and chamber before heating to 1350 °C at a rate of 4 °C/s, and then to 1600 °C at a rate of 1 °C/s. The sample was held for 30 s before cooling to 1200 °C at 1 °C/s, and they let naturally cool to room temperature. This was repeated with a 10 °C/s cooling rate from 1600 °C to 1200 °C. All tests were repeated at least once for each sample and condition.

3. Results and discussion

As a benchmark Fig. 2 shows the DSC cooling curves for both the pure iron and the low carbon steel. This was measured at 0.5 °C/s in a NETZSCH STA 449 F3 *Jupiter* DSC which is the top end of the achievable cooling rates in this model. It can be seen that the liquidus temperature for the pure iron and low carbon steel is 1520 and 1495 °C respectively. The onset of delta ferrite to austenite transformation occurs at 1425 °C.

Fig. 3a shows the measured radiated heat taken from a pixel from the surface of the molten sample during cooling at 1 °C/s of a pure iron sample. The temperature plotted is the recorded temperature measured by a type R thermocouple integrated in the crucible holder. It is observed that a linear decline in radiated heat can be seen initially. At 26 s the heat emitted then starts to rise and is consistent with the start of solidification. In this case solidification will have started subsurface and therefore increasing the temperature of liquid at the surface of the droplet, this can be seen in Fig. 3b-2 where the surface is still liquid (it should be noted that during the test an obvious change in the convention of the sample was observed in real time). At 50 s there is a sharp spike in radiated heat, this is likely to be attributed to the surface emissivity decrease from liquid steel to solid steel [16], with CSLM observation agreeing to this (Fig. 3b-3). After this a continual decrease in the radiated heat is seen. Using the CSLM temperature measurement then solidification in this case occurred between 1522 and 1495 °C. This is in good agreement with the DSC trace shown in Fig. 2 which showed a solidification range of 1520 to 1495 °C. It should be noted however, unlike the DSC, enthalpy of fusion cannot be calculated from these curves as heat is not only lost from the surface, but also conducted through the crucible, and the proportion of this balance is not known.

As such a large change in the signal was seen at the latter stages of solidification (which is consistent with the surface solidifying) then the same analysis was used on a pixel in the crucible base, 0.5 mm away from the droplet (Fig. 4). This curve shows a similar trace but without the final spike, this agrees well that the spike is attributed to a change in surface emissivity as the crucible will not undergo any significant changes in emissivity. The change in radiated heat here is therefore attributed to the conduction from the sample as the latent heat is given off during the droplets transformation. The significant temperatures are consistent between both sets of data.

In both Figs. 3 and 4 the red arrows depict the temperature at which solidification is predicted to start under equilibrium conditions [17]. It can be seen that in general there is good agreement allowing for a small degree of undercooling to occur.

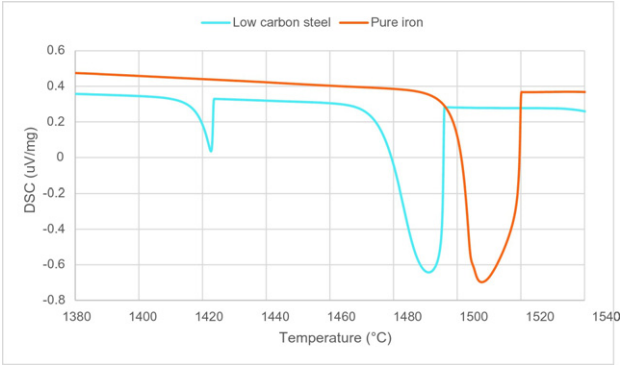

Fig. 2. DSC traces during cooling at 0.5 °C/s for the pure iron and low carbon steel used in this study.